A resource for the development of methodologies for lung nodule size estimation: database of thoracic CT scans of an anthropomorphic phantom[◊]

Marios A Gavrielides[1*], Lisa M Kinnard[1,2], Kyle J Myers[1], Jennifer Peregoy[3], William F Pritchard[3], Rongping Zeng[1], Juan Esparza[3], John Karanian[3], and Nicholas Petrick[1]

[1]*Division of Imaging and Mathematics, Office of Science and Engineering Laboratories, Center for Devices and Radiological Health, U.S. Food and Drug Administration, Silver Spring, MD*
[2]*Currently with the Congressionally Directed Medical Research Program, Fort Detrick, MD*
[3]*Laboratory of Cardiovascular and Interventional Therapeutics, Division of Biology, Office of Science and Engineering Laboratories, Center for Devices and Radiological Health, U.S. Food and Drug Administration, Silver Spring, MD*

marios.gavrielides@fda.hhs.gov

Abstract: A number of interrelated factors can affect the precision and accuracy of lung nodule size estimation. To quantify the effect of these factors, we have been conducting phantom CT studies using an anthropomorphic thoracic phantom containing a vasculature insert to which synthetic nodules were inserted or attached. Ten repeat scans were acquired on different multi-detector scanners, using several sets of acquisition and reconstruction protocols and various nodule characteristics (size, shape, density, location). This study design enables both bias and variance analysis for the task on nodule size estimation. The resulting database provides a publicly available resource to facilitate the assessment of lung nodule size estimation methodologies.

OCIS codes: 110.6955 Tomographic imaging 110.1758 Computational imaging 110.7440 X-ray imaging 110.6880 Three-dimensional image acquisition

[◊]**Datasets associated with this article are available at** http://midas.osa.org/midaspre/midas/item/view/871?key=a3dySERwN3FUaG9SYw==.

References

1. P. Therasse, S. G. Arbuck, E. A. Eisenhauer, J. Wanders, R. S. kaplan, L. Rubinstein, J. Verweij, M. V. Glabbeke, A. T. v. Oosterom, M. C. Christian, and S. G. Gwyther, "New guidelines to evaluate the response to treatment in solid tumors," Journal of the National Cancer Institute **92**, 205-216 (2000).
2. E. A. Eisenhauer, P. Therasse, J. Bogaerts, L. H. Schwartz, D. Sargent, R. Ford, J. Dancey, S. Arbuck, S. Gwyther, M. Mooney, L. Rubinstein, L. Shankar, L. Dodd, R. Kaplan, D. Lacombe, and J. Verweijk, "New response evaluation criteria in solid tumours: Revised RECIST guideline (version 1.1)," European Journal of Cancer **45**, 228-247 (2009).
3. C. C. Jaffe, "Measures of response: RECIST, WHO, and new alternatives," Journal of Clinical Oncology **24**, 3245-3251 (2006).
4. M. A. Gavrielides, L. M. Kinnard, K. J. Myers, and N. Petrick, "Non-calcified lung nodules: Volumetric assessment with thoracic CT," Radiology **251**, 1-11 (2009).
5. C. R. Meyer, S. G. A. III, C. P. Fenimore, G. McLennan, L. M. Bidaut, D. P. Barboriak, M. A. Gavrielides, E. F. Jackson, M. F. McNitt-Gray, P. E. Kinahan, N. Petrick, and B. Zhao, "Quantitative Imaging to assess tumor response to therapy: common themes, of measurement, truth data, and error sources," Translational Oncology 2, 198-210 (2009).

6. M. Das, J. Ley-Zaporozhan, H. A. Gietema, A. Czech, G. Muhlenbruch, A. H. Mahnken, M. Katoh, A. Bakai, M. Salganicoff, S. Diederich, M. Prokop, H. U. Kauczor, R. W. Gunther, and J. E. Wildberger, "Accuracy of automated volumetry of pulmonary nodules across different multislice CT scanners," Eur Radiol **17**, 1979- 1984 (2007).
7. W. J. Kostis, A. P. Reeves, D. F. Yankelevitz, and C. I. Henschke, "Three- dimensional segmentation and growth-rate estimation of small pulmonary nodules in helical CT images," IEEE Trans Med Imaging **22**, 1259-1274 (2003).
8. L. M. Kinnard, M. A. Gavrielides, K. J. Myers, R. Zeng, J. Peregoy, W. Pritchard, J. Karanian, and N. Petrick, "Volume Error Analysis for Lung Nodules Attached to Bronchial Vessels in an Anthropomorphic Thoracic Phantom", Proc. SPIE **6915**, 69152Q1-69152Q9 (2008).
9. M. A. Gavrielides, R. Zeng, L. M. Kinnard, K. J. Myers, and N. Petrick, "A template-based approach for the analysis of lung nodules in a volumetric CT phantom study," Proc. SPIE **7260**, 7260091- 72600911 (2009).
10. M. A. Gavrielides, R. Zeng, L. M. Kinnard, K. J. Myers, and N. Petrick, Division of Imagjng and Applied Mathematics, OSEL?CDRH?FDA are preparing a manuscripy to be called "Estimation of lung nodule size in a phantom CT study using a matched filter approach".

1. Introduction

Technological advances in computer tomography (CT) over the last decade have enabled the acquisition of thin (less than 1mm), near isotropic thoracic scans in a single breath hold. These advances can potentially improve temporal CT analysis so that the detection of small (less than 1cm in diameter) lung nodules can be obtained and changes in nodule size can be assessed early. These improvements have lead to an improved ability to both diagnose disease and to characterize the response of tumors to therapy so that the proper treatment for individual patients can be administered. Change in lesion size is one approach for estimating drug response, however it assumes that bias (difference between measured and true size) is constant along temporal scans. If this assumption does not hold, then evaluating the change in measured lesion size between scans in problematic. An approach that quantifies size specific to the CT hardware and scan parameters before a comparison would be preferred in order to correctly account for these biases.

Currently, lung nodule size is typically assessed using the RECIST criteria [1, 2], which are based on the measurement of the maximum diameter of a nodule from a single slice. The RECIST criteria suffer from certain limitations [3], the most important of which is the assumption of nodule sphericity. Volumetric assessment of nodule size has been investigated as an approach that is better suited to the true representation of lung nodule shape due to its use of 3D data. However, a number of factors can affect the precision and accuracy of volumetric CT for the estimation of lung nodule size, as was summarized in a recent review article [4]. These factors include acquisition and reconstruction parameters, nodule characteristics, and the performance and usage of measurement tools. We have been conducting phantom studies to quantify the effect of such factors with an overall goal of developing methods to account for errors in lung nodule volumetry. Phantom studies provide a framework in which the true size, shape, and location of nodules is known, allowing for bias analysis. Moreover, they allow for the acquisition of multiple scans required for variance analysis, which would be more difficult to acquire in human studies because of the additional radiation exposure to patients. Additionally phantom data may serve as a means for directly comparing the performance of different nodule sizing algorithms on a fixed set of phantom nodules [5].

In order for findings from phantom studies to be applicable to clinical data, phantoms should be somehow representatives of actual lung nodules, and should also incorporate the complexity of the surrounding background and interfering vessel structures. State-of-the-art thoracic phantoms incorporating lung vasculature are now available and, while not completely matching the characteristics of a clinical scan, they do a much better job of synthesizing the

variability coming from the vascular nature of the lung field. Synthetic nodules can be attached to the vasculature of such a thoracic phantom to approximate the complexity of clinical nodules; studies have shown that the performance of segmentation algorithms is significantly lower for cases of attached nodules [6-8]. Synthetic nodules with irregular shapes and margins, as well as inhomogeneous densities to mimic non-solid nodules can be manufactured. Scans of these anthropomorphic phantoms and synthetic nodules can be used in the development and evaluation of methodologies for non-solid nodule size estimation. Currently, there is a lack of methods in the literature addressing such methodologies [4].

In our phantom studies we have employed an anthropomorphic thoracic phantom with a vasculature insert to which synthetic nodules with characteristics that span the range of clinical nodules can be attached or inserted. The thoracic phantom has been scanned using multiple scanners and imaging protocols to examine the effect of scanner model, acquisition, and reconstruction parameters on lung nodule size estimation. Each imaging protocol and nodule layout has been scanned repeatedly (10 repeats) to enable variance analysis in addition to bias analysis.

Using a systematic approach to probe the factors that may affect the precision and accuracy in lung nodule estimation, we have collected a vast amount of phantom CT data. This data is in the process of becoming publicly available as a resource to enable developers to perform comparisons between different methods regarding measurement error. This resource can complement public databases of clinical datasets such as the Reference Image Database for Evaluation of Response (RIDER) consortium and the Lung Image Database Consortium (LIDC) database, created by the National Cancer Institute (NCI) and the National Institute of Biomedical Imaging and Bioengineering (NIBIB). In this manuscript the aforementioned phantom CT database is described in detail.

2. Database Description

2.1 Anthtropomorhic phantom

The anthropomorphic thoracic phantom (Kyotokagaku Incorporated, Tokyo, Japan) employed in this study is shown in Figure 1, along with the vasculature insert. Thus far we have acquired scans with nodules attached to the vasculature as well as scans with nodules inserted without attachment to vessels by placing them in low-density foam. The phantom does not contain lung parenchyma so the space within the vascular structure is filled with air.

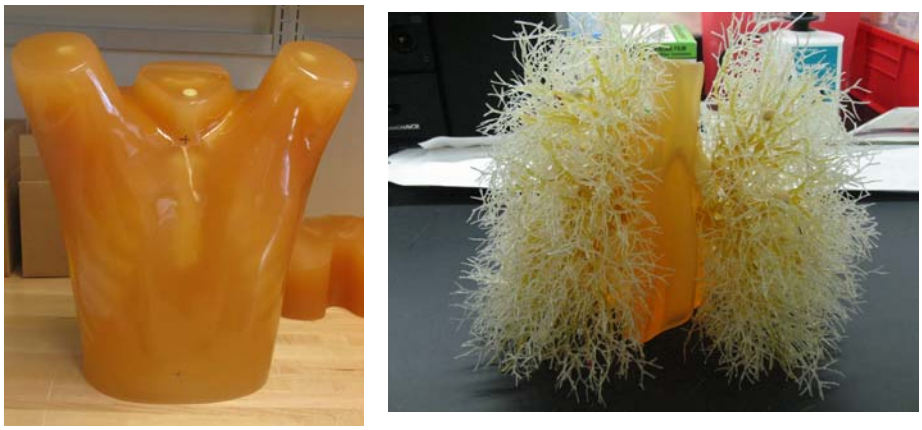

Fig 1: Photograph of the exterior shell of the thoracic phantom (left) and the vasculature insert (right).

2.2 Synthetic lung nodules

The set of synthetic lung nodules used in this study were independently manufactured by Kyotokagaku Incorporated (Japan) and Computerized Imaging Reference Systems (CIRS, Norfolk, VA). They consisted of objects varying in size (5, 8, 10, 12, 20, 40 mm), shape (spherical, elliptical, lobulated, spiculated), and density (-800, -630, -10, +100 HU). Figure 2 shows samples of synthetic nodules in various sizes and shapes.

Figure 2: Photographs of the different types of synthetic nodules used in this study. Each column shows nodules in three sizes, starting with spiculated on the left, lobulated in the center, and elliptical on the right. The three sizes shown here were manufactured to have the equivalent volumes of spherical nodules with diameters of 1.0, 2.0, and 4.0mm respectively.

Eight different layouts of nodules were specified by placing them in premarked positions within the phantom vasculature, where they were either attached to vessels or suspended in foam (non-attached configuration). Care was taken to maintain constant positioning of the nodules when a particular layout was scanned multiple times or with different protocols. For that purpose, vessels on which nodules were attached were color coded. Table I tabulates the nodule configuration for each layout in terms of nodule positioning, size, shape, and density. Figure 3 shows an example diagram of one layout used in this study.

Nodule layout	**Vessel attachment**	**Nodule placement and description**					
		Left lung			**Right lung**		
		Size	*Shape*	*HU*	*Size*	*Shape*	*HU*
1	attached	5,8,10	spherical	-630	5,8,10	spherical	-800
2	attached	8,10,12	irregular	-630	5,8,10	spherical	+100
3	attached	5,8,10, 20, 40	spherical	-630	5,8,10, 20, 40	spherical	+100
4	attached	10, 20	elliptical lobulated, spiculated	-630	10, 20	elliptical lobulated, spiculated	+100
5	attached	40	spiculated	-630	40	spiculated	+100
6	attached	5,8,10, 20, 40	spherical	-10	20, 40	spherical	-630, +100
7	attached	10, 20	elliptical lobulated, spiculated	-10	5,8	elliptical lobulated, spiculated	-10
8	non-attached	5,8,10	spherical	-630, +100	5,8,10	spherical	-800, -10

Future additions to the set of nodules (currently under construction) will include non-homogeneous objects (i.e., an object of 5 mm in size and -630 HU in density, enclosed in a 10mm object of -10HU). Different combinations of sizes and densities are being manufactured to more closely mimic non-solid or part-solid nodules as well as nodules surrounded by inflammation and nodules with necrotic centers.

A key component of the CT lung phantom project is the ability to compare the estimated nodule size with the known *true* size or reference gold standard. As part of our project, volume was used as a surrogate measure of size. The true volume estimate of each synthetic nodule was derived from weight and density measures. Both the CIRS-and Kyotokagaku nodules were accompanied by density measures. Nodule weights were measured in our lab using a precision scale of 0.1 mg tolerance (Adventurer Pro AV 2646, Ohaus Corp, Pine Brook, NJ). Three repeat weight measurements were made and these weights were averaged to produce a final estimated weight for each nodule.

2.3 Scan acquisition and reconstruction parameters

The phantom was scanned using a Philips 16-row scanner (Mx8000 IDT, Philips Healthcare, Andover, MA) and a Siemens 64-row scanner (Somatom 64, Siemens Medical Solutions USA, Inc., Malvern, PA). Scans were acquired with varying combinations of effective dose, pitch, and slice collimation, and were reconstructed with varying combinations of slice thicknesses and reconstruction kernels. Examples of such scans are shown in Figures 4 and 5. Ten exposures were acquired for each imaging protocol. The phantom position was not changed during the 10 repeat exposures; however it was repositioned between different imaging protocols or different nodule layouts.

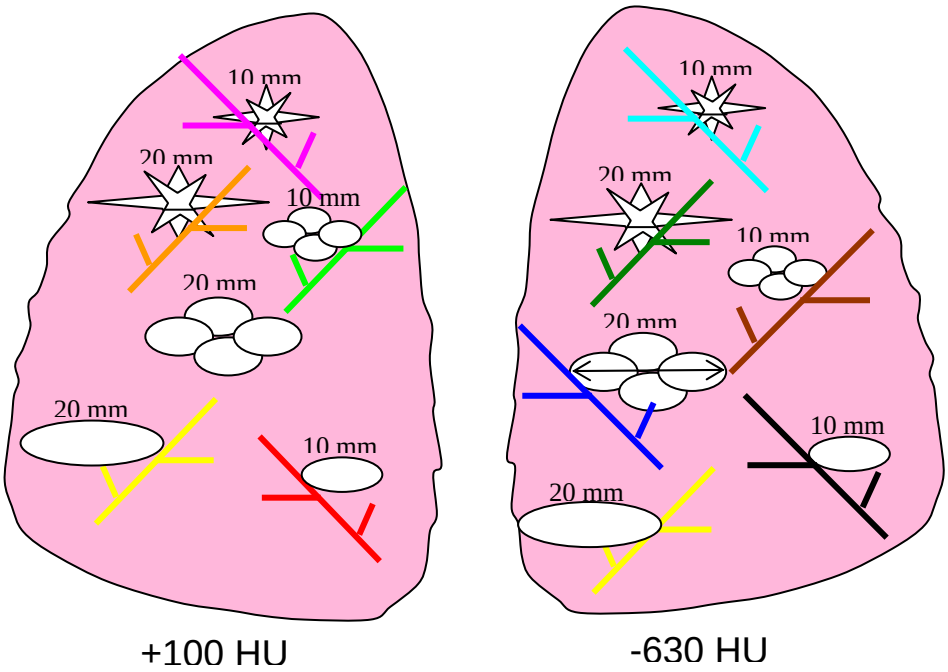

Figure 3. An example layout (Layout #4) indicating the positioning of each nodule along with information on the size, shape, and density of each nodule in the layout. Vessel branches within the anthropomorphic phantom were color coded for the purpose of mapping nodules to specific positions within the phantom's vasculature structure in a reproducible manner.

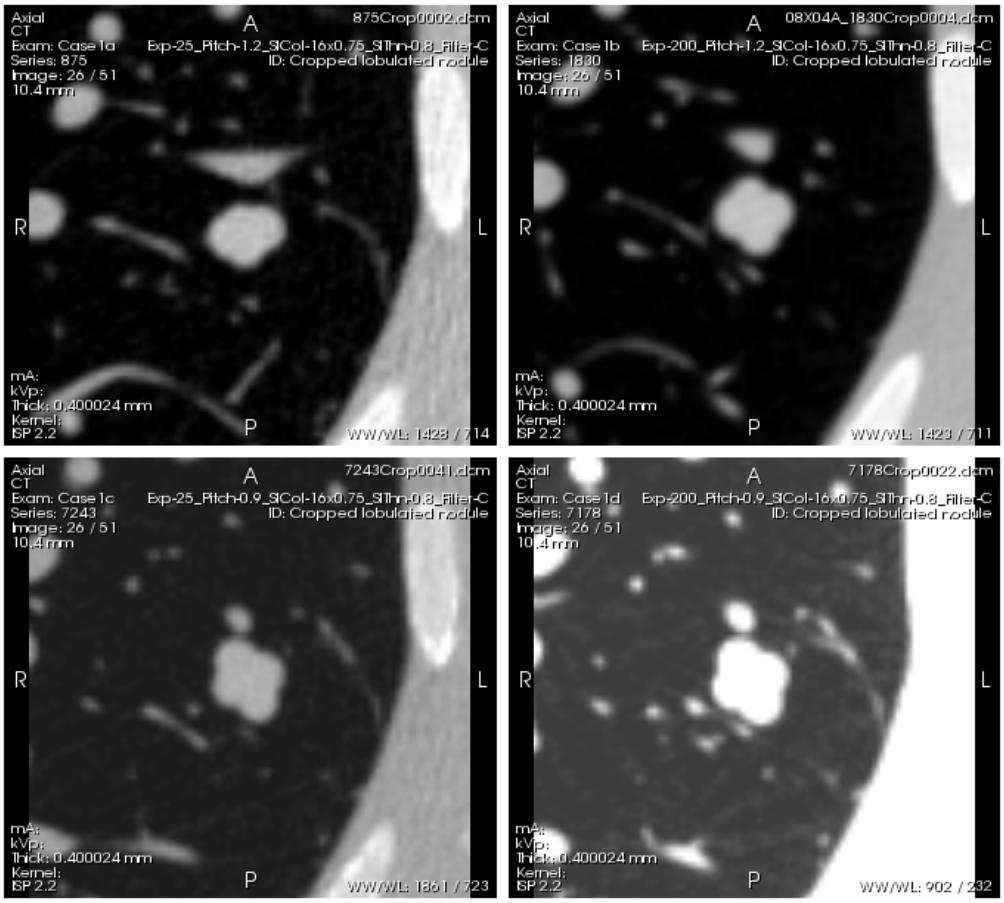

Figure 4. Example scans of a lobulated nodule of -10HU density and 10mm equivalent diameter (volume equal to the one of a spherical nodule of 10mm diameter), acquired with the following 4 different protocols: *Top left (Case 1a)*- low dose (25mAs), 1.2 pitch. *Top right (Case 1b)*- high dose (200mAs), 1.2 pitch. *Bottom left (Case 1c)*- low dose (25mAs), 0.9 pitch. *Bottom right (Case 1d)*- high dose (200mAs), 0.9 pitch. The whole series of each scan can be viewed by clicking on the Interactive Science Publishing (ISP) hyperlink (View 1).

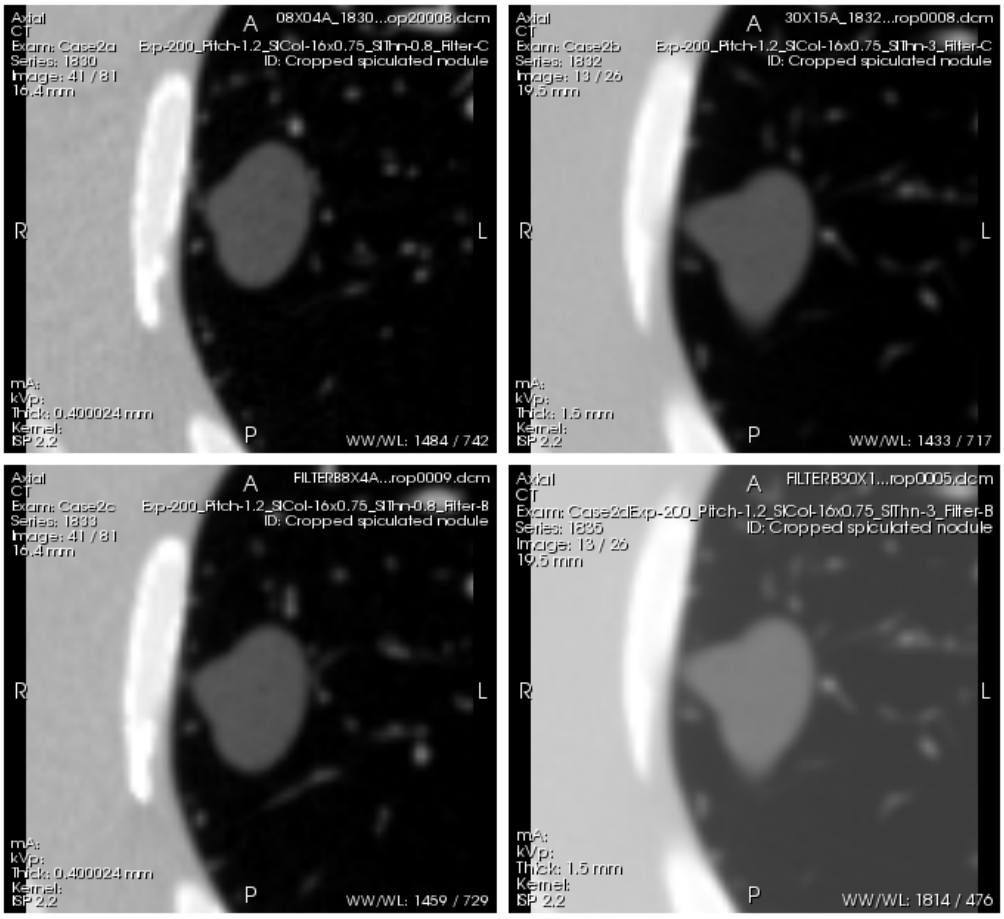

Figure 5. Example scans of a spiculated nodule of -630HU density and 20mm equivalent diameter (volume equal to the one of a spherical nodule of 20mm diameter), acquired with the following 4 different protocols: *Top left (Case 2a)*- thin slice thickness (0.8mm), detail reconstruction kernel (BF60). *Top right (Case 2b)*- thick slice thickness (3.0mm), detail reconstruction kernel (BF60). *Bottom left (Case 2c)*- thin slice thickness (0.8mm), medium reconstruction kernel (BF40). *Bottom right (Case 2d)*- thick slice thickness (3.0mm), medium reconstruction kernel (BF40). All scans were acquired with a high dose (200mAs) and 1.2 pitch. The whole series of each scan can be viewed by clicking on the Interactive Science Publishing (ISP) hyperlink (View 2).

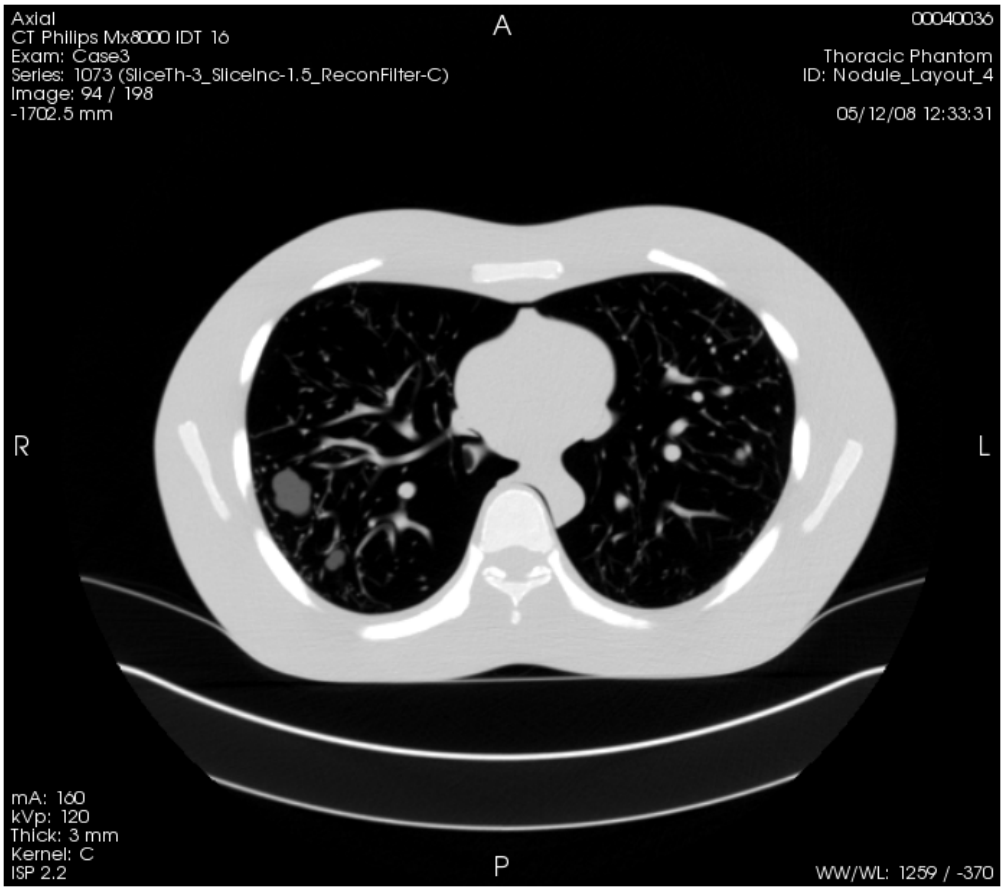

Figure 6. Example series of Layout 4, acquired with 100mAs and reconstructed to 3mm. The whole series can be viewed by clicking on the Interactive Science Publishing (ISP) hyperlink (View 3).

Nodule Layout, Scanner	Eff.dose (mAs)	Slice collimation (mm)	Slice overlap	Pitch	Recon. Slice thickness (mm)	Recon. Kernels	# sets
1, S1	20,100,200	16x0.75, (16x1.5)	50%	0.9,1.2	0.75,1.5,3 (2,3,5)	detail	**360**
2, S1	20,100,200	16x0.75, (16x1.5)	50%	0.9,1.2	0.75,1.5,3 (2,3,5)	detail, medium	**720**
3, S1	20,100,200	16x0.75, (16x1.5)	50%	0.9,1.2	0.75,1.5,3 (2,3,5)	detail, medium	**720**
3, S2	20,100,200	64x0.6	0%, 50%	0.9,1.2	0.75,1.5,3	detail, medium	**720**
4, S2	20,100,200	16x0.75, (16x1.5)	0%, 50%	0.9,1.2	0.75,1.5,3 (2,3,5)	detail, medium	**720**
5, S2	20,100,200	16x0.75, (16x1.5)	50%	0.9,1.2	0.75,1.5,3 (2,3,5)	detail, medium	**360**
6, S2	20,100,200	16x0.75, (16x1.5)	50%	1.2	0.75,1.5,3 (2,3,5)	detail, medium	**360**
7, S2	20,100,200	16x0.75, (16x1.5)	50%	0.9,1.2	0.75,1.5,3 (2,3,5)	detail, medium	**720**
8, S2	20,100,200	16x0.75, (16x1.5)	50%	0.9,1.2	0.75,1.5,3 (2,3,5)	detail, medium	**720**
TOTAL							**5400**

Table II. Summary of reconstructed CT datasets: a description of the individual nodule layouts are provide in Table I. *S1: 16-row Philips Mx8000 IDT (Philips Healthcare, Andover, MA), S2: 64-row Siemens Somatom Definition (Siemens Medical Solutions USA, Inc., Malvern, PA).

3. Results and Discussion

Table II summarizes the acquired CT scan data at the moment of publication by specifying the layout and scanner and imaging parameters for each dataset. More than 1500 reconstructed CT scans are currently available. All scans can be obtained from the National Biomedical Imaging Archive (NBIA)[1]. As mentioned previously, the specific nodules (size, shape, density, attachment) within each layout are tabulated in Table I. As an example, Figure 6 shows a slice data from a high exposure (200mAs), thick slice (3.0mm) scan of Layout 4.

The database described in this manuscript can serve as a publicly available resource for a number of different applications in the field of thoracic CT imaging. Primarily, it is well-suited for the development and assessment of methodologies for lung nodule size estimation. Both bias and variance analysis of nodule sizing can be obtained using this phantom database because the reference standard (i.e., truth nodule size) and repeat exposures for each configuration are included in the database. This is the main advantage of such phantom data over clinical data, where the true size or extent of nodule is unknown and repeat scans are difficult to justify because of the radiation exposure. The phantom database can serve in a complementary role to existing or developing clinical databases such as the Reference Image Database for the Evaluation of Response (RIDER).[2]

Even though the phantom lacks the complexity of human lung anatomy, the wide range in size, shape, and density of the synthetic nodules and the presence of the vasculature structure can be useful in providing important information on the performance of and comparison between nodule size estimators. A number of studies have used phantom studies for lung nodule measurement but all have used their own phantoms, making it difficult to compare results across methodologies; this database provides a common framework for such comparisons. It has already been employed in two projects, namely the VOLCANO'09[3] and BIOCHANGE[4]. The VOLCANO'09 competition is part of the Second International Workshop of Pulmonary Image Analysis with a goal to compare the outcomes of various algorithms measuring the change in volume of pulmonary nodules in CT scans using a common dataset and performance evaluation method. CT data from our phantom and synthetic nodules was included in the competition dataset along with clinical data provided by the Weill Medical College of Cornell University. The BIOCHANGE 2008 project was organized by the National Institute of Standards and Technology (NIST) as a benchmarking pilot study of lung CT change measurement algorithms and computer-aided diagnosis tools. In related work Kinnard et al. [8] have reported on volumetric analysis results comparing different 3D segmentation algorithms.

Another use of the phantom CT database is the development and optimization of lung nodule estimation methodologies. Recent work by co-authors of this study [9, 10] included the development of a matched-filter approach for the estimation of lung nodules. The matched filter minimized a cost function between the lung nodule to be measured and a bank of simulated 3D nodule templates. The simulated templates were generated using a model of the helical MDCT imaging system, which included a forward projection and filtered back projection-based image reconstruction and derived simulated reconstructed data of nodule objects (templates) of varying size. The templates were then matched to CT data of the target nodules to derive the estimate of the scanned nodule size. The phantom CT database was

[1] https://cabig.nci.nih.gov/tools/NCIA
[2] https://wiki.nci.nih.gov/display/Imaging/RIDER
[3] http://www.via.cornell.edu/challenge/
[4] http://www.itl.nist.gov/iad/894.05/biochange2008/Biochange2008-webpage.htm

used to compare cost functions and assess the performance of this method. Results demonstrated the effect of vessel attachments, nodule characteristics, and imaging protocols on volumetric precision and accuracy, supporting the value of the database to provide lower bounds on performance.

In addition to lung nodule size estimation, the phantom CT scan database can be used in a number of other applications in thoracic CT imaging such as the analysis of helical CT noise to derive useful properties such as noise correlation. Understanding noise properties is necessary for developing signal-detection theoretic estimators that make optimal use of the deterministic and stochastic processes of the image formation process. The database provides a large number of regions of interest from CT scans acquired with multiple imaging parameters that can be used for noise analysis. Other applications may include the development and evaluation of 3D algorithms for segmenting the lung field or the lung vasculature.

4. Conclusions

We have collected multiple CT datasets using a factorial design across image acquisition parameters and nodule characteristics using a well-characterized phantom and a variety of imaging platforms. The data will be available publicly as a resource to examine the impact of numerous CT acquisition parameters and data analysis approaches on the accuracy and precision of tumor size estimates and to facilitate the development of procedures that will maximize the utility of CT imaging for lung cancer screening and tumor therapy evaluation.

Acknowledgments

This research was funded though a Critical Path grant from the U.S. Food and Drug Administration. The intramural research program of the National Institute of Biomedical Imaging and Bioengineering and the National Cancer Institute through IAG no. 224-07-6030 also provided partial support for this work. Phantom scans on the Siemens Somatom Definition were conducted at the Center for Clinical Imaging Research in the Mallinckrodt Institute of Radiology (MIR) at the Washington University School of Medicine in St. Louis, MO. The authors would like to thank Bruce Whiting of MIR for his assistance.

Disclaimer:

The mention of commercial products, their sources, or their use in connection with material reported herein is not to be construed as either an actual or implied endorsement of such products by the Department of Health and Human Services.